

# Deconfinement<sup>1</sup>

C. Pajares

*Instituto Galego de Física de Altas Enerxías, Departamento de Física de Partículas.  
Universidade de Santiago de Compostela. 15782 Santiago de Compostela, Spain.*

## Abstract.

This is an attempt to summarize the talks given at the session on Deconfinement in the Conference “Quark Confinement and hadron spectrum”. This talk covers the following topics: Elliptic flow and evidence of nearly perfect fluid of the created matter; High Transverse momentum production, propagation of jets and energy loss; Heavy quarkonia in dense QCD matter; Phase transition, Multiplicity fluctuations and long range correlations; Multiparticle production and thermalization.

**Keywords:** <Enter Keywords here>

**PACS:** <Replace this text with PACS numbers; choose from this list:

In the last few years a large progress has been done in the knowledge of the deconfined phase of QCD. The SPS data already displayed several facts that hinted at the onset of Quark Gluon Plasma (QGP) formation. The RHIC data have conclusively discovered a striking set of new phenomena. Most of these data have been extensively discussed in the different talks of the session of Deconfinement.

The space limits prevent me from describing all the reported exciting developments, so I will concentrate on some of them.

## ELLIPTIC FLOW

The flow pattern of thousand of particles produced in a heavy ion reaction is the main observable used to look for collective behaviour and its properties. These properties test the conditions necessary for the obtention of QGP. One is the degree of thermalization. The evolution of the matter from the initial conditions can be computed by means of relativistic hydrodynamics if local equilibrium is maintained. These equations can be further approximated by perfect fluid equation when the viscosity correction can be neglected. The second condition is the validity of the equation of state, numerically determined from QCD. The data on elliptic flow show evidence that a fast thermalization is reached at RHIC energy, compatible with a soft equation of state and a low viscosity. The matter created at RHIC behaves as a perfect fluid [1].

The elliptic flow,  $v_2 = \langle p_x^2 - p_y^2 / p_t^2 \rangle$ , results from pressure gradients developed in the initial almond-shaped collision zone. That is, the initial transverse coordinate

---

<sup>1</sup> Summary of the Deconfinement Session of the Quark Confinement and Hadron Spectrum VII Conference. Ponta Delgada, Azores(Portugal)

space anisotropy of the collision zone or eccentricity  $\varepsilon = \langle (y^2 - x^2)/(y^2 + x^2) \rangle$  is converted, via hadronic or partonic interactions into an azimuthal momentum anisotropy. Elliptic flow self-quenches due to expansion of the collision zone, therefore in order to achieve relatively large  $v_2$  a fast thermalization is required (see Lisa and Bai-Yuting talks [2] and [3]). Therefore it is expected that the elliptic flow scaled by the eccentricity should be proportional to the density of scatterings,  $\frac{1}{S} \frac{dN}{dy}$ , being  $S$  the overlapping collision area. This is well satisfied as fig. 1 shows. It is also shown the hydrodynamics result for a perfect fluid [4], which only is reached for central Au-Au collisions. As a for LHC, for central Au-Au collisions  $\frac{1}{S} \frac{dN}{dy} \simeq 80$  it is expected a change on the shape of the curve becoming flat. In fig. 2 we show the agreement of the observed hadron mass dependence of  $v_2$  with the hydrodynamics predictions below  $p_t = 1$  GeV/c. This result shows that there is a common collective flow velocity. In fig. 3 it is shown the scaling law of  $v_2/n$  versus  $p_T/n$ ,  $n$  being the number of quarks of the respective hadrons. This scaling law was predicted by coalescence models suggesting that the collective flow is at the partonic stage. The coalescence models, also explain naturally the differences between the inclusive cross sections for baryons and mesons at intermediate transverse momentum as it was explained in the Hippolyte talk [5]. The hydrodynamics perfect fluid prediction [6] for the higher azimuthal momentum  $v_4$  is  $v_4 = \frac{1}{2}v_2^2$ , but the data for  $\pi^\pm$  and  $p$  and  $\bar{p}$  in minimum bias Au-Au collisions gives a factor 3/2 instead 1/2. However in a perfect fluid model [7] it is obtained the scaling law  $v_4 = v_2^2/2 + k_4 y_T^4$ , which is in agreement with data.  $k_4$  is a constant depending on the mass of the particle and  $y_T = \frac{1}{2} \log(m_T + p_T)/(m_T - p_T)$ .

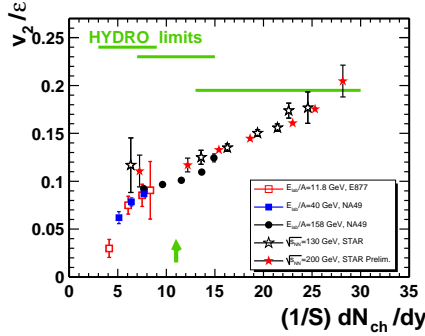


**FIGURE 1.**  $\frac{v_2}{\varepsilon}$  versus  $\frac{1}{S} \frac{dN_{ch}}{dy}$  for different energies and centralities.

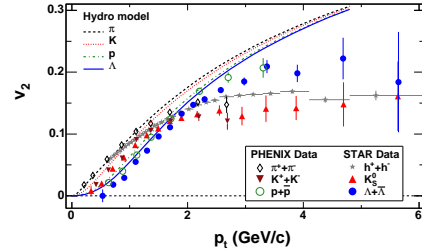


**FIGURE 2.** The elliptic flow  $v_2$  versus  $p_T$  for different particles together with the hydrodynamics model predictions

## TRANSVERSE MOMENTUM SUPPRESSION

One of the exciting results of the RHIC data is the strong suppression of  $p_T$  in central heavy ion collisions, consistent with the predicted energy loss [8] [9] of the parent light quarks and gluons when transverse the dense colored medium due to the induced gluon radiation. In fig. 4 is shown the nuclear attenuation factor  $R_{AA}(p_T)$ . For  $\pi^0$  and  $\eta$  the data show a suppression factor 5 for  $p_T > 4$  GeV/c, compared to the superposition of  $NN$  collision, see N. Borghini talk [10]. On the contrary,  $R_{AA} = 1$  for direct photons in agreement with perturbative QCD [11] [12].

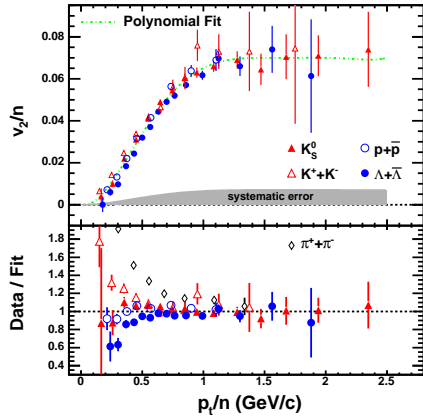


**FIGURE 3.**  $\frac{v_2}{n}$  versus  $\frac{p_T}{n}$  being  $n$  the number of quark constituents for different mesons and baryons

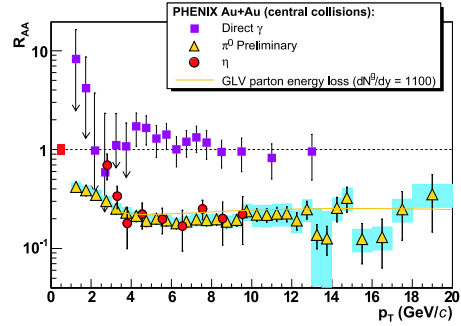


**FIGURE 4.** PHENIX data for central Au-Au collisions of the modified nuclear factor  $R_{AA}$  as a function of transverse momentum for photons,  $\pi$  and  $\eta$

However, the suppression factor for high  $p_T$  electrons from semi-leptonic D and B decays is as suppressed as the light hadrons in central Au-Au collision [13], see fig. 5, in conflict with the prediction of radiative energy loss models. This discrepancy may point out to a elastic energy loss for heavy quarks. The study of b and c jets at LHC can be very valuable to clarify this point.

A second exciting phenomena observed at RHIC was the suppression of the back to back jet-like correlation. Jet-like correlations are measured by selecting the highest  $p_T$  trigger hadron of the event and measuring the azimuthal  $\Delta\Phi = \Phi - \Phi_{trig}$  and rapidity  $\Delta\eta = \eta - \eta_{trig}$  distributions of associated hadrons. In  $pp$  collisions a dijet signal appears as two back to back Gaussian peaks at  $\Delta\Phi \simeq 0$  (near-side) and  $\Delta\Phi \simeq \pi$  (away-side). On the contrary, the away-side dihadron azimuthal correlation in central Au-Au collision is clearly suppressed, showing a dip and a double peak structure [14] at  $\Delta\Phi \approx \pi \pm 1.1$ , for associated hadron in the range  $1 \leq p_T \leq 2.5 \text{ GeV}/c$  (see fig. 6). This double peak structure has been pointed out as due to the emission of energy from the quenched parton at a finite angle respect to the jet axis. Such conical configuration can appear if a fast jet moving in a fluid medium generates a wake of shock wave of Mach Type [15] or Cerenkov Type [16]. In the case of Mach wave, the characteristic angle  $\theta$  of the emitted secondaries determines the speed of sound,  $c_s = \cos\theta$ . However the double-peak structure of the away-side correlation is consistent not only with conical emission but also with other scenarios. In order to distinguish between the different mechanisms, 3-particle azimuthal correlations are needed. The three particle results reported at this conference [17] as central Au-Au collisions are consistent with conical emission, but additional studies on the  $p_T$  dependence are needed to emission distinguish between Mach cone shock waves and Cerenkov emission.

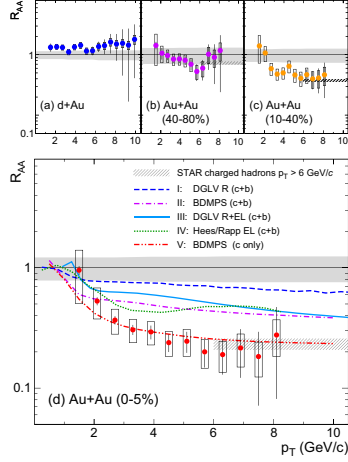


**FIGURE 5.**  $R_{AA}$  versus  $p_T$  for nonphotonic electrons for d-Au (a), Au-Au 40-80 (b), Au-Au 10-40 (c) and Au-Au 0-5 (d) compared with the STAR data for charged hadrons

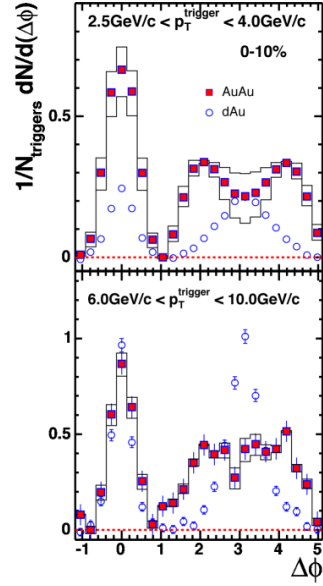


**FIGURE 6.** STAR data on azimuthal distributions of semihard hadrons (associated  $p_T = 1 - 2.5$  GeV/c) in central Au-Au and d-Au collisions with respect to a trigger hadron measured of  $2.5$  GeV/c  $< p_T < 4.0$  GeV/c (top) and  $6.0$  GeV/c  $< p_T < 10.0$  GeV/c.

## CHARMONIUM SUPPRESSION

Early predictions were that the two heavy quarks that would form the bound state would be screened from each other in the high-density deconfined medium [18]. These states would melt at different energy densities depending on their size and binding energies. However, recently, lattice QCD has suggested that the  $J/\psi$  would not be screened up to  $T \geq 1.5 - 2T_c$ . On the contrary other charmonium states would be screened around  $1.1T_c$  [19].

The  $J/\psi$  suppression at RHIC was predicted to be larger than the observed at SPS by most of the models. Contrary to this expectation, additional suppression was not found, fig. 7. In this figure it is also shown the suppression due to normal absorption using for the absorption cross section the values 1, 3 and 4 mb respectively. The usual used value of 4.2 mb is higher than the required by  $d - Au$  data which is in the range 1-3 mb. A better understanding of the absorption cross section and in general of cold nuclear matter effects would be welcome.

We are left with two possible theoretical explanations of the RHIC data, namely regeneration [22] and sequential dissociation [23] models. In regeneration models a strong dissociation of the charm pairs due to screening is compensated by the regeneration of bound charm pairs in the later states of the expansion due to the large production of charmed quarks at high density. At LHC a large enhancement is predicted.

In the sequential screening model, the  $J/\psi$  is not melt at SPS and RHIC energies as suggested by lattice calculations and the observed suppression comes only from

screening of the higher mass resonances  $\psi'$  and  $\chi_c$  that though feed down normally provide about 40% of the  $J/\psi$  production. This picture provides a simple explanation for the similar suppression observed at SPS and RHIC. As at LHC it would be reached temperatures high enough to dissociate  $J/\psi$ , it is expected stronger suppression at LHC, contrary to the regeneration model expectation.

On the other hand, the sequential dissociation model relates the observed  $J/\psi$  production to the higher resonance production once the absorption has been subtracted. In fact, denoting by  $S_{J/\psi}$  and  $S_{\psi'}$ , the survival probabilities for the observed total suppression and for the higher resonances respectively, once the absorption has been subtracted

$$S_{J/\psi} = 0.6 + 0.4S_{\psi'} \quad (1)$$

Using the absorption cross sections  $\sigma_{\psi'} = 7.1 \pm 1.6 \text{ mb}$  and  $\sigma_{J/\psi} = 4.3 \pm 0.3 \text{ mb}$  we can test the equation (1) from the data on  $J/\psi$  and  $\psi'$  production, obtaining a good agreement

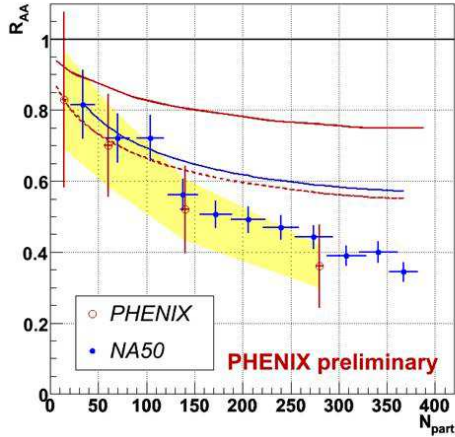


**FIGURE 7.** NA50 data together with PHENIX data of the modified nuclear factor  $R_{AA}$  for  $J/\psi$  production as a function of the number of participants.

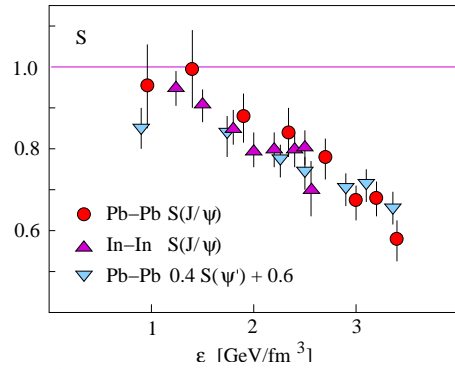


**FIGURE 8.** The survival probability of  $J/\psi$  for Pb-Pb and In-In collisions together with expression (1).

## PHASE TRANSITION

Lattice studies indicate that the deconfinement phase transition at  $\mu = 0$  is a cross over [24], as at  $\mu \neq 0$  it is expected to be of first order, in some point there will be a critical end point. At this conference, were reported studies both experimental and theoretical on this critical end point. From one side, it was explained the proposal RHICII [25] which will explore regions of lower energy, looking for signatures associated to the critical point. In this way, it will join FAIR in the search of the critical point. On the other hand were reported interesting theoretical results. B. Kaempfer [26] in a quasi-particle model on of QCD matter study the critical end point and the equation of state, obtaining with agreement for relevant observables of AA collisions as the elliptical flow for different particles or the rapidity multiplicity distribution. Szabo reported the recent results of lattice at  $\mu$  and  $\mu \neq 0$ , in particular the cross-over at  $\mu = 0$ . Antonov analytically studied [27] thermodynamics of a heavy quark-antiquark pair in SU(3) QCD, both below

and above the deconfinement critical temperature. He derived the effective temperature-dependent string tension, which enabled him to calculate internal energy and entropy of two heavy-light mesons for two flavours. The anomalously large peaks of these two observables around  $T_c$ , observed recently on the lattice are well described.

Other interesting aspects of the phase transition (dynamics, flux-tube) were discussed by G. Krein [28] and G. Kozlov [29].

## CORRELATIONS

In the early stage of heavy ion collision an extended region with large energy density is produced where quark and gluons degrees of freedom leading to a new partonic phase of matter. In the subsequent evolution, the system dilutes and cools down, hadronizes and finally decays into observed hadrons. These hadrons carry only indirect information about the early stage of the collision. Results as the elliptic flow discussed before suggest that a deconfined phase starts in the early stage of the reaction. The study of correlation and fluctuations can provide additional information on the reaction mechanism. For these reasons correlations between oppositely charge particles and multiplicity and transverse momentum fluctuations have been measured in the last years.

The balance function [30] measured the correlation of the oppositely charged particles. The width of the balance function  $\langle \Delta y \rangle$  is sensitive to the hadronization time.

If the system produced in a heavy-ion collision has undergone a partonic phase, the hadronization will occur at later time and therefore the temperature will be lower and the diffusive interaction with other particles will be lesser than those in the direct hadronization [31]. A delayed hadronization implies stronger correlation in rapidity for the charged particles and therefore a narrower balance function. Indeed a narrowing of the balance function is observed with increasing size of the colliding nuclei by the NA49 and STAR Collaboration [32]. The Hijing model as well as shuffled events retaining only correlations from global charge conservation do not show any decrease of the width. However, other models without delayed hadronization can describe the data [33]. Notice, that the integral of the balance function is related to the event by event charge fluctuations, which are expected to be suppressed in a QGP [34].

The multiplicity correlations have been studied by the NA49 Correlations [35]. In fig. 9, the scaled variance of negative particles is shown as a function of the number of projectile participants together with the results of three different string models. It has been pointed out that for peripheral collisions a significant contribution comes from fluctuations in the number of target participants at fixed projectile participant number, what means that the projectile and target hemisphere are connected. The strings models of fig. 9 are based on Fritiof model where the strings are stretched between partons of the same excited hadron and therefore there is not connection between hemispheres. This does not happen in string models like, dual parton model, quark gluon string model and Venus where there is color exchange and the strings are stretched between partons of the projectile and the target.

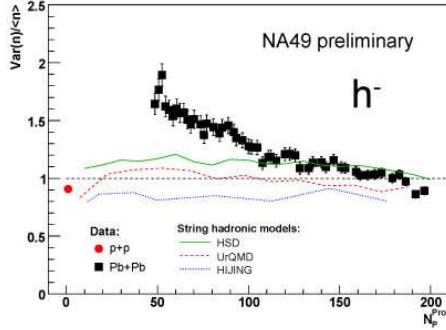


**FIGURE 9.** NA49 experimental data on the scaled variance of negative multiplicity of Pb-Pb collisions as a function of the number of projectile participants together the predictions of different non color exchange string models.

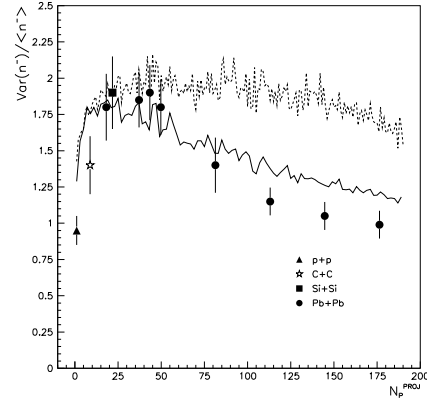


**FIGURE 10.** NA49 preliminary data on scaled variance of negative multiplicity as a function of the number of projectile participants compared with the result of percolation of strings.

In fig. 10 it is shown the result of a percolation color sources model [37] together with previous NA49 data. It is seen that contrary to the above string models in this case reproduced the general trend of data. The percolation framework is able to describe the dependence on the centrality of the transverse momentum fluctuations [38]. In this approach the strings stretched between partons of the projectile and target. In the transverse space these color strings are seen as small circles, with  $r_0 \simeq 0.2 - 0.3 fm$ . With growing energy and/or atomic number, the number of strings grows, starting to overlap forming clusters. Each cluster decay into particles with a mean multiplicity and mean transverse momentum which depends on the number of strings of the cluster and the total area of the cluster. These dependence are essentially determined by the Schwinger mechanism and the color field of each cluster. At a certain critical density, a macroscopic cluster appear which marks the percolation phase transition [39]. The fluctuations are understood as follows: At low density, most of the particles are produced by individual strings with the same mean multiplicity and mean  $p_T$ , therefore small fluctuations. At large density above the critical point essentially there will be only are cluster and therefore the fluctuations are small. The maximum of fluctuations corresponds to the largest number of clusters with different size and number of strings.

The percolation of strings predicts that the long range rapidity correlation measured by  $D_{FB}^2 = \langle n_B n_F \rangle - \langle n_F \rangle \langle n_B \rangle$  (between forward F and backward B the rapidity gap should be larger than 1-1.5 to eliminate short range correlations) increases with centrality, being much less than what is expected from superposition models [40]. This is in agreement with STAR preliminary data [41].

In Color Glass Condensate (CGC) [42] we expect also that  $D_{FB}^2$  grows with the centrality [43]. In fact, the main contribution is given by

$$\langle \frac{dN}{dy_1} \frac{dN}{dy_2} \rangle \simeq \langle \left( \frac{dN}{dy} \right)^2 \rangle \simeq \frac{1}{\alpha_s^2} \pi R^2 Q_s^2 \quad (2)$$

As centrality increases,  $\alpha_s$  decreases and (2) grows.

## THERMALIZATION

It is clear that a fast thermalization of the partonic is required. We learned at beginning of the conference [44] that this can be achieved naturally in the CGC approach. In this approach, the collision of two heavy ion, which are gluon saturated in the initial state, develop strong longitudinal chromoelectric fields [45], which via the Schwinger mechanism produce particles with a thermal spectrum due to the fluctuations of the color field. The temperature  $T$  of this spectrum is related to the saturation momentum  $Q_s$ ,  $T \simeq Q_s/2\pi$ . The thermalization time is  $\tau \sim 1/Q_s$ .

As it has pointed out [44], a similar picture arises in percolation [46]. In this case, the critical density  $\eta_c$  for the non-thermal percolation phase can be related to the critical temperature,  $T_c = \frac{\langle p_T \rangle_1}{\sqrt{2F(\eta_c)}}$ , where  $\langle p_T \rangle_1$  is the mean transverse momentum of particles produced in one single string (essentially the string tension) and  $F(\eta_c) = \sqrt{\frac{1-e^{-\eta_c}}{\eta_c}}$  has geometrical origin and has to do with the fraction of total available area occupied by the cluster  $(1 - e^{-\eta_c})$ . The shear viscosity is  $\langle p_T \rangle_1 F(\eta)L$  is also determined by the same factor.  $L$  is the longitudinal extension,  $L \simeq 1 fm$ . For reasonable values of  $\langle p_T \rangle_1 \simeq 200 MeV$  and  $\eta_c \simeq 1.2 - 1.5$ , it is obtained  $T_c = 170 - 180 MeV$  and a very low shear viscosity.

In conclusion, theoretical and experimental progress have been achieved in the understanding of deconfinement as it has been reported in the different talks of this session. The future experiments of LHC, FAIR and we expect that also RHIC II will let us to go on this understanding, and clarify some of the questions of the field.

## ACKNOWLEDGMENTS

We thank the organizers for such a nice meeting and Y. Foka, J. Rafelski and M. Leith for helping in the configuration of this talk. The work has done under contract FPA2005-01963 of SPAIN and the support of Xunta de Galicia.

## REFERENCES

1. M. Gyulassy and L. McLerran, *Nucl. Phys. A* **750**, 30 (2005).
2. M. Lisa, this conference.
3. Bai Yuting, this conference.
4. D. Teaney, J. Lauren and E. V. Shuryak, nucl-th/0110037.
5. B. Hippolyte, this conference.
6. N. Borghini and J. Y. Ollitrant, *Phys. Lett. B*, to appear.
7. R. Lacey, *Nucl. Phys. A* **774**, 199 (2006).



8. J. D. Bjorken, Fermilab-Pub 82-059-THY; M. Gyulassy, M. Plumer, M. Thoma and X. N. Wang, *Nucl. Phys. A* **538**, 37c (1992).
9. R. Baier, Y. L. Dokshitzer, A. H. Mueller and D. Schiff, *JHEP***109**, 033 (2001).
10. N. Borghini, this conference.
11. K. Reygers, this conference.
12. H. Torii, this conference.
13. S. S. Adler et al., PHENIX nucl-ex/010047; J. Bielcik et al., STAR nucl-ex/051105.
14. S. S. Adler et al., PHENIX nucl-ex/0507004.
15. H. Stocker, *Nucl. Phys. A* **750**, 121 (2005); J. Casalderrey, E. Shunyak, D. Teaney, *J. Phys. Conf. Ser.* **27** 22 (2005).
16. V. Koch, A. Majumder and X. N. Wang, *Phys. Rev. Lett.* **96**, 172302 (2006); I. M. Dremin, *Nucl. Phys. A* **767**, 233 (2006).
17. F. Wong, STAR Collaboration. This conference and nucl-ex/0610027.
18. T. Matsui and H. Satz, *Phys. Lett. B* **178**, 416 (1986).
19. F. Karsch, *Eur. Phys. J. C* **43**, 35 (2005).
20. M. Leith, this conference, nucl-ex/0610031.
21. P. Martins, NA60 Collaboration, this conference.
22. L. Grandchamp, R. Rapp and G. E. Brown, *Phys. Rev. Lett.* **92**, 212301 (2004); R. L. Thews, *Eur. Phys. J. C* **43**, 97 (2005).
23. F. Karsch, D. Kharzeev and H. Satz, *Phys. Lett. B* **637**, 75 (2006).
24. Y. Aoki, G. Endrodi, Z. Fodor, S. D. Katz and K. K. Szabo, *Nature* **443**, 675 (2006); K. K. Szabo, this conference.
25. D. Gabor, this conference.
26. B. Kampfer, this conference; M. Bluhm and B. Kampfer, hep-ph/0511015.
27. D. Antonov, this conference.
28. G. Krein, this conference.
29. G. Kozlov, this conference.
30. P. Christakoglou, this conference.
31. S. A. Bass, P. Danielewicz and S. Pratt, *Phys. Rev. Lett.* **85**, 2689 (2000).
32. C. Alt et al., NA49 Collaboration, *Phys. Rev. C* **71**, 034903 (2005).
33. D. Jiaxin, L. Na and L. Lianshou, nucl-th/0606062.
34. V. Koch, M. Bleicher and S. Jeon, *Nucl. Phys. A* **698**, 261 (2002).
35. B. Lungwitz, this conference.
36. M. Bleicher, this conference.
37. E. G. Ferreira, this conference; L. Cunqueiro, E. G. Ferreira, F. del Moral and C. Pajares, *Phys. Rev. C* **72**, 024907 (2005).
38. E. G. Ferreira, F. del Moral and C. Pajares, *Phys. Rev. C* **69**, 034901 (2004).
39. M. A. Braun, N. Armesto, E. G. Ferreira and C. Pajares, *Phys. Rev. Lett* **77**, 3736 (1996); M. Nardi and H. Satz, *Phys. Lett. B* **442**, 14 (1998).
40. N. A. Amelin, et al., *Phys. Rev. Lett.* **73**, 2813 (1984); S. Hanssler, M. Abdel-Aziz and M. Bleicher, nucl-th/0608075.
41. T. Tarnowsky, STAR Collaboration, nucl-ex/0606018.
42. E. Iancu, this conference.
43. N. Armesto, L. McLerran and C. Pajares, hep-ph/0607245 *Nucl. Phys. A* to appear.
44. D. Kharzeev, this conference; D. Kharzeev, E. Levin, K. Tuchin, hep-ph/0602063; D. Kharzeev, K. Tuchin, *Nucl. Phys. A* **753**, 316 (2005).
45. T. Lappi and L. McLerran, *Nucl. Phys. A* **722**, 200 (2006).
46. J. Dias de Deus and C. Pajares, *Phys. Lett. B* **642**, 455 (2006).